Ain Shams Engineering Journal (2014) 5, 691–702

Ain Shams University

Ain Shams Engineering Journal

www.elsevier.com/locate/asej
www.sciencedirect.com

ELECTRICAL ENGINEERING

# Dynamic stability enhancement of power system based on a typical unified power flow controllers using imperialist competitive algorithm

M.R. Banaei [a,*], S.J. Seyed-Shenava [b], Parisa Farahbakhsh [b]

[a] Department of Electrical Engineering, Azarbaijan Shahid Madani University, Tabriz, Iran
[b] Department of Electrical Engineering, University of Mohaghegh Ardabili, Ardabil, Iran

Received 16 October 2013; revised 20 December 2013; accepted 16 January 2014
Available online 7 March 2014

KEYWORDS
UPFC;
Imperialist competitive algorithm;
Damping controller

**Abstract** This paper presents dynamic model of power system installed with a novel UPFC that consist of two shunt converters and a series capacitor. In this configuration, a series capacitor is used between two shunt converters to inject desired series voltage. As a result, it is possible to control the active and reactive power flow. The main advantage of the proposed UPFC in comparison with the conventional configuration is injection of a series voltage waveform with a very low total harmonic distortion (THD). In addition, a linearized Phillips–Heffron model is obtained and a supplementary controller for the modeling of proposed UPFC to damp low frequency oscillations with considering four alternative damping controllers is recommended. The problem of robustly novel UPFC based damping controller is formulated as an optimization problem according to the time domain-based objective function, which are solved using particle swarm optimization (PSO) and Imperialist Competitive Algorithm (ICA) techniques.


## 1. Introduction

Presently, power demand is growing considerably and the extension in transmission and generation is restricted with the rigid environmental constraints and limited availability of resources. Consequently, power systems of today are much more loaded than before. This brings about the essential for power systems to be operated near their stability limits. Moreover, interconnection between remotely located power systems gives rise to low-frequency oscillations in the range of 0.1–0.3 Hz. These oscillations may keep growing in magnitude, resulting in a loss of synchronism, if not well damped [1].

Power system stabilizers (PSSs) have been used to serve the purpose of increasing power system damping to low frequency oscillations. PSSs have proved to be efficient in performing their assigned tasks. A wide range of PSS tuning approaches has been recommended. These approaches have included pole placement [2], damping torque concepts [3], $H_\infty$ [4], variable

* Corresponding author. Tel.: +98 9144017344; fax: +98 4124327566.
E-mail addresses: m.banaei@azaruniv.ac.ir (M.R. Banaei), parisafarahbakhsh@gmail.com (P. Farahbakhsh).
Peer review under responsibility of Ain Shams University.

Production and hosting by Elsevier

2090-4479 © 2014 Production and hosting by Elsevier B.V. on behalf of Ain Shams University.
http://dx.doi.org/10.1016/j.asej.2014.01.003

structure [5], and the different optimization and artificial intelligence techniques [6–8]. However, PSS may adversely affect voltage profile and may not be able to arrest oscillations resulting from severe disturbances, such as three-phase faults at generator terminals [9].

Recently FACTS controllers such as UPFC and STATCOM and IPFC have been applied for damping oscillations and improving dynamic stability of power systems [10]. FACTS devices, when used to improve power system steady-state performance, have shown very promising results. Through the modulation of bus voltage, phase shift between buses, and transmission line reactance, FACTS devices can cause a robust increase in power transfer limits during steady-state. Because of the extremely fast control action connected with FACTS-device operations, they have been very encouraging applicants for utilization in power system damping enhancement. It has been observed that employing a feedback supplementary control, in addition to the FACTS-device primary control, can considerably enhance system damping and can also improve system voltage profile, which is advantageous over PSSs [11].

Among them, UPFC is impressive for damping power system oscillations. This is obtained by regulating the controllable parameters of the system, line impedance, voltage magnitude and phase angle of the UPFC bus. The UPFC consists of two AC/DC converters. One of the two converters is connected to the transmission line via a series transformer and the other in parallel with the line via a shunt transformer. The series and shunt converters are connected via a large DC capacitor. The series branch of the UPFC injects an AC voltage with controllable magnitude and phase angle at the power frequency via an insertion transformer [12]. Recently researchers have presented dynamic models of UPFC in order to design suitable controller for power flow, voltage and damping controls [13–17]. Wang has presented a modified linearized Phillips–Heffron model of a power system installed with UPFC [18,19]. He has addressed the basic issues relating to design UPFC damping controllers, i.e., selection of robust operating conditions for designing damping controllers; and the election of parameters of UPFC (such as $m_E$, $m_B$, $\delta_E$ and $\delta_B$) to be modulated for achieving desired damping. Wang has not presented a systematic approach for designing the damping controllers. Further, no attempt seems to have been made to identify the most suitable UPFC control parameters, in order to arrive at a robust damping controller and he has not used the deviation of active and reactive powers, $\Delta P_e$ and $\Delta Q_e$ as the input control signals. Abido has used the control PSO, for designing controller and this manner not only is an off-line procedure, but also depends strongly to selection of primary conditions of control system [20,7].

Recently, the intelligent techniques are used for optimal tuning of UPFC based damping controller. These techniques are used in multiple applications, such as PID controller designing, optimal placement of FACTS devices, economic load dispatch of power systems, power system stabilization, or harmonic omission in multilevel inverters. Among the intelligent algorithms PSO and ICA are used.

In [21] has been proposed a novel configuration of UPFC which consists of two shunt converters and a series capacitor. The injected series voltage waveform by this configuration has extremely low THD. The proposed UPFC is based on using only two 2-level 3-phase shunt converters and a series capacitor. So, the cost, volume and rated power of UPFC decrease and the control scheme becomes simpler than conventional UPFC configuration. In the proposed configuration, left shunt converter supplies to or absorbs from utility the necessary active power to regulate the voltage of dc link capacitor. It also exchanges reactive power with utility to control the sending end reactive power. It can be noted that the operation of this converter is same as shunt converter in conventional UPFC. On the other hand, right shunt converter tracks reference current to control the current of series capacitor to inject the desired series voltage, $V_{se}$. It should be noted that the proposed configuration is able to have all of the capabilities of conventional UPFC. Its reason is that the main functions of conventional UPFC are injecting the desired series voltage by series converter and tracking the reference current by shunt converter in order to exchange the active and reactive powers while both of these functions exist in proposed configuration of UPFC because it is possible to inject the series voltage with any desired amplitude and phase angle by combination of series capacitor and right shunt converter operation as well as to track the reference current by left shunt converter to have the same operation of shunt converter of conventional configuration.

In this paper, a connected single machine to infinite bus with novel UPFC, which consists of two shunt converters and a series capacitor installed, is used and a novel linearized Phillips–Heffron model for the mentioned power system is derived for design of the UPFC damping controller. In addition, the particle swarm optimization (PSO) and the Imperialist Competitive Algorithm (ICA) are used for the optimal tuning of the proposed UPFC based damping controller in order to enhance the damping of a power system's low-frequency oscillations and achieve the desired level of robust performance under different operating conditions, as well as different parameter uncertainties and a disturbance.

## 2. Description of case study system

Fig. 1 shows a SMIB power system equipped with the proposed configuration of UPFC which consists of two shunt converters and a series capacitor. The synchronous generator is transferring power to the infinite-bus through a transmission line and a UPFC. The UPFC consists of two excitation transformers, a series capacitor, two three-phase IGBT based voltage source converters, and a DC link capacitors.

First shunt converter, in the proposed configuration, supplies to or absorbs from utility the necessary active power to regulate the voltage of dc link capacitor. It also trades reactive

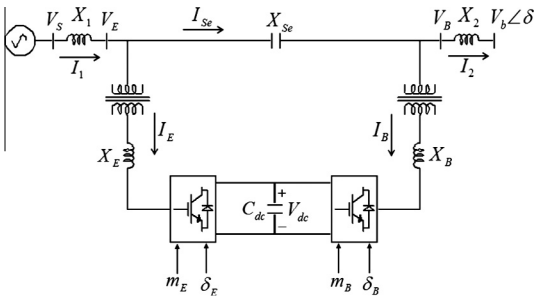


**Figure 1** SMIB power system equipped with proposed UPFC.

power with utility to control the sending end reactive power. It can be noted that the operation of this converter is same as shunt converter in conventional UPFC. On the other hand, second shunt converter tracks reference current to control the current of series capacitor to inject the desired series voltage, $V_{se}$. It should be noted that the proposed configuration is able to have all of the capabilities of conventional UPFC. In this study, the four input control signals to the proposed UPFC are $m_E$, $m_B$, $\delta_E$, and $\delta_B$.

## 3. Dynamic model of proposed UPFC

### 3.1. Power system nonlinear

The dynamic model of the UPFC that is shown in Fig. 1, is required in order to study the effect of the UPFC for enhancing the small signal stability of the power system. The system data are given in the Appendix A. By applying Park's transformation and neglecting the resistance and transients of transformers, the UPFC can be modeled as:

$$\begin{bmatrix} V_{Ed} \\ V_{Eq} \end{bmatrix} = \begin{bmatrix} 0 & -X_E \\ X_E & 0 \end{bmatrix} \begin{bmatrix} I_{Ed} \\ I_{Eq} \end{bmatrix} + \frac{m_E V_{dc}}{2} \begin{bmatrix} \cos(\delta_E) \\ \sin(\delta_E) \end{bmatrix} \tag{1}$$

$$\begin{bmatrix} V_{Bd} \\ V_{Bq} \end{bmatrix} = \begin{bmatrix} 0 & -X_B \\ X_B & 0 \end{bmatrix} \begin{bmatrix} I_{Bd} \\ I_{Bq} \end{bmatrix} + \frac{m_B V_{dc}}{2} \begin{bmatrix} \cos(\delta_B) \\ \sin(\delta_B) \end{bmatrix} \tag{2}$$

$$\dot{V}_{dc} = \frac{3m_E}{4C_{dc}} [\cos(\delta_E) \quad \sin(\delta_E)] \begin{bmatrix} I_{Ed} \\ I_{Eq} \end{bmatrix} + \frac{3m_B}{4C_{dc}} [\cos(\delta_B) \quad \sin(\delta_B)] \begin{bmatrix} I_{Bd} \\ I_{Bq} \end{bmatrix} \tag{3}$$

The complete dynamic model of a single-machine infinite-bus power system equipped with the proposed UPFC can be developed by combining (1–3) with the machine dynamic equations shown below:

$$\dot{\delta} = \omega_0 \omega \tag{4}$$

$$\dot{\omega} = \frac{P_m - P_e - D\omega}{M} \tag{5}$$

$$\dot{E}'_q = \frac{-E_q + E_{fd}}{T'_{d0}} \tag{6}$$

$$\dot{E}_{fd} = -\frac{1}{T_A} E_{fd} + \frac{K_A}{T_A} (V_{s0} - V_s) \tag{7}$$

where

$$\begin{aligned} &T_e = P_e = V_{sq} I_{1q} + V_{sd} I_{1d}, \\ &E_q = E'_q + (X_d - X'_d) I_{1d}, \ V_s = \sqrt{V_{sd}^2 + V_{sq}^2}, \\ &V_{sd} = X_q I_{1q}, \ V_{sq} = E'_q - X'_d I_{1d}, \ I_{1d} = I_{sed} + I_{Ed}, \\ &I_{1q} = I_{seq} + I_{Eq} \end{aligned}$$

Also, for the estimated power system model, from Fig. 1. We have:

$$\begin{aligned} &V_S = jX_1 I_1 + V_E \\ &V_E = V_{se} + jX_2 I_2 + V_b \angle \delta \\ &V_{se} = V_E - V_B = -jX_{se} I_{se} \\ &V_B = jX_2 I_2 + V_b \angle \delta \end{aligned} \tag{8}$$

From above equations, line currents can be obtained as:

$$I_{sed} = -\frac{X_E}{X_{se}} I_{Ed} + \frac{X_B}{X_{se}} I_{Bd} - \frac{m_E \sin(\delta_E) V_{dc}}{2X_{se}} + \frac{m_B \cos(\delta_B) V_{dc}}{2X_{se}} \tag{9}$$

$$I_{seq} = -\frac{X_E}{X_{se}} I_{Eq} + \frac{X_B}{X_{se}} I_{Bq} + \frac{m_E \cos(\delta_E) V_{dc}}{2} - \frac{m_B \sin(\delta_B) V_{dc}}{2} \tag{10}$$

$$I_{Ed} = \frac{X_{1d}}{X_{d\sum}} E'_q + \frac{X_{EEd}}{X_{d\sum}} \frac{m_E \sin(\delta_E) V_{dc}}{2} + \frac{X_{EBd}}{X_{d\sum}} \times \frac{m_B \sin(\delta_B) V_{dc}}{2} + \frac{X_{2d}}{X_{d\sum}} V_b \cos(\delta) \tag{11}$$

$$I_{Eq} = \frac{X_{EEq}}{X_{q\sum}} \frac{m_E \cos(\delta_E) V_{dc}}{2} + \frac{X_{EBq}}{X_{q\sum}} \frac{m_B \cos(\delta_B) V_{dc}}{2} + \frac{X_{1q}}{X_{q\sum}} V_b \sin(\delta) \tag{12}$$

$$I_{Bd} = \frac{X_{3d}}{X_{d\sum}} E'_q + \frac{X_{BEd}}{X_{d\sum}} \frac{m_E \sin(\delta_E) V_{dc}}{2} + \frac{X_{BBd}}{X_{d\sum}} \times \frac{m_B \sin(\delta_B) V_{dc}}{2} - \frac{X_{4d}}{X_{d\sum}} V_b \cos(\delta) \tag{13}$$

$$I_{Bq} = \frac{X_{BEq}}{X_{q\sum}} \frac{m_E \cos(\delta_E) V_{dc}}{2} + \frac{X_{BBq}}{X_{q\sum}} \frac{m_B \cos(\delta_B) V_{dc}}{2} - \frac{X_{2q}}{X_{q\sum}} V_b \sin(\delta) \tag{14}$$

$$I_{1d} = E'_q \cdot \frac{X_{t1}}{X_{Se} X_{d\sum}} + m_E \sin(\delta_E) V_{dc} \cdot \frac{X_{t2}}{2X_{Se} X_{d\sum}} - m_B \sin(\delta_B) V_{dc} \cdot \frac{X_{t3}}{2X_{Se} X_{d\sum}} + V_b \cos(\delta) \cdot \frac{X_{t4}}{X_{Se} X_{d\sum}} \tag{15}$$

$$I_{1q} = m_E \cos(\delta_E) V_{dc} \cdot \frac{X_{t5}}{2X_{Se} X_{q\sum}} + m_B \cos(\delta_B) V_{dc} \cdot \frac{X_{t6}}{2X_{Se} X_{q\sum}} + V_b \sin(\delta) \cdot \frac{X_{t7}}{X_{Se} X_{q\sum}} \tag{16}$$

### 3.2. Power system linearized model

A linear dynamic model is obtained by linearizing the nonlinear model round an operating condition. The linearized model of power system is given as follows:

$$\Delta\dot{\delta} = \omega_b \Delta\omega \tag{17}$$

$$\Delta\dot{\omega} = \frac{\Delta P_m - \Delta P_e - D\Delta\omega}{M} \tag{18}$$

$$\Delta\dot{E}'_q = \frac{-\Delta E_q + \Delta E_{fd} + (X_d - X'_d)\Delta I_{1d}}{T'_{do}} \tag{19}$$

$$\Delta\dot{E}_{fd} = \frac{-\Delta E_{fd} + K_A(\Delta V_{ref} - \Delta V_S + \Delta u_{pss})}{T_A} \tag{20}$$

$$\Delta\dot{V}_{dc} = K_7 \Delta\delta + K_8 \Delta E'_q - K_9 \Delta V_{dc} + K_{CE} \Delta m_E + K_{C\delta_E} \Delta\delta_E + K_{CB} \Delta m_B + K_{C\delta_B} \Delta\delta_B \tag{21}$$

The equations below can be obtained with a line arising from (17–21).

$$\Delta P_e = K_1\Delta\delta + K_2\Delta E'_q + K_{Pdc}\Delta V_{dc} + K_{PE}\Delta m_E + K_{P\delta_E}\Delta\delta_E + K_{PB}\Delta m_B + K_{P\delta_B}\Delta\delta_B \quad (22)$$

$$\Delta E_q = K_4\Delta\delta + K_3\Delta E'_q + K_{qdc}\Delta V_{dc} + K_{qE}\Delta m_E + K_{q\delta_E}\Delta\delta_E + K_{qB}\Delta m_B + K_{q\delta_B}\Delta\delta_B \quad (23)$$

$$\Delta V_S = K_5\Delta\delta + K_6\Delta E'_q + K_{Vdc}\Delta V_{dc} + K_{VqE}\Delta m_E + K_{V\delta_E}\Delta\delta_E + K_{VB}\Delta m_B + K_{V\delta_B}\Delta\delta_B \quad (24)$$

The state-space equations of the system can be calculated by combination of (22–24) with (17–21):

$$\dot{X} = AX + BU$$

$$X = [\Delta\delta, \Delta\omega, \Delta E'_q, \Delta E_{fd}, \Delta V_{dc}]^T \quad (25)$$

$$U = [\Delta u_{pss}, \Delta m_E, \Delta\delta_E, \Delta m_B, \Delta\delta_B]^T$$

$$A = \begin{bmatrix} 0 & \omega_b & 0 & 0 & 0 \\ -\frac{K_1}{M} & -\frac{D}{M} & -\frac{K_2}{M} & 0 & -\frac{K_{Pdc}}{M} \\ -\frac{K_4}{T'_{do}} & 0 & -\frac{K_3}{T'_{do}} & \frac{1}{T'_{do}} & -\frac{K_{qdc}}{T'_{do}} \\ -\frac{K_A K_5}{T_A} & 0 & -\frac{K_A K_6}{T_A} & -\frac{1}{T_A} & -\frac{K_A K_{Vdc}}{T_A} \\ K_7 & 0 & K_8 & 0 & -K_9 \end{bmatrix} \quad (26)$$

$$B = \begin{bmatrix} 0 & 0 & 0 & 0 & 0 \\ 0 & -\frac{K_{PE}}{M} & -\frac{K_{P\delta_E}}{M} & -\frac{K_{PB}}{M} & -\frac{K_{P\delta_B}}{M} \\ 0 & -\frac{K_{qE}}{T'_{do}} & -\frac{K_{q\delta_E}}{T'_{do}} & -\frac{K_{qB}}{T'_{do}} & -\frac{K_{q\delta_B}}{T'_{do}} \\ \frac{K_A}{T_A} & -\frac{K_A K_{VqE}}{T_A} & -\frac{K_A K_{V\delta_E}}{T_A} & -\frac{K_A K_{VB}}{T_A} & -\frac{K_A K_{V\delta_B}}{T_A} \\ 0 & K_{CE} & K_{C\delta_E} & K_{CB} & K_{C\delta_B} \end{bmatrix} \quad (27)$$

Where $\Delta m_E$, $\Delta m_B$, $\Delta\delta_E$ and $\Delta\delta_B$ are a linearization of the input control signal of the UPFC and the equations related to the $K$ parameters have been presented in Appendix B. The linearized dynamic model of (21–24) can be seen in Fig. 2, where there is only one input control signal for $\Delta u$. Fig. 2 includes the UPFC relating the pertinent variables of electric torque, speed, angle, terminal voltage, field voltage, flux linkages, UPFC control parameters and dc link voltage.

## 4. PSO and ICA

### 4.1. Particle swarm optimization

Particle swarm optimization (PSO) was introduced first in [22]. PSO approach features many advantages; it is simple, fast and can be coded in few lines. Also, its storage requirement is minimal.

PSO starts with a population of random solutions "particles" in a D-dimension space. The $i$th particle is represented by $X_i = (x_{i1}, x_{i2}, \ldots, x_{iD})$. PSO consists of, at each step, changing the velocity of each particle toward its $p_{best}$ and $g_{best}$ according to Eq. (28). The velocity of particle $i$ is represented as $V_i = (v_{i1}, v_{i2}, \ldots, v_{iD})$. The position of the $i$th particle is then updated according to Eq. (29).

$$v_{id} = \omega v_{id} + c_1 r_1(p_{id} - x_{id}) + c_2 r_2(p_{gd} - x_{gd}) \quad (28)$$

$$x_{id} = x_{id} + v_{id} \quad (29)$$

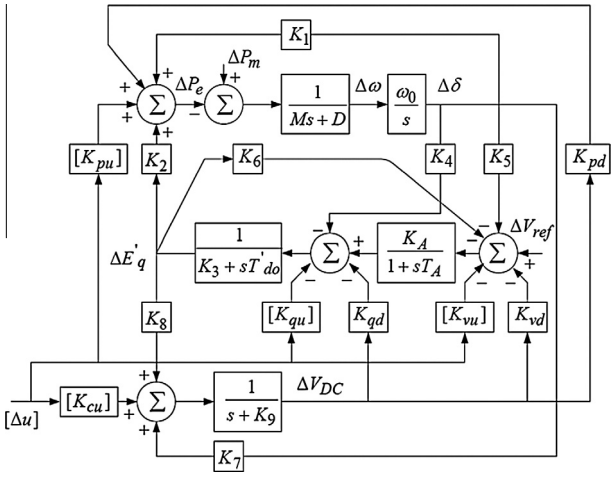


**Figure 2** Modified Heffron–Phillips transfer function model.

*where*, $p_{id} = p_{best}$ *and* $p_{gd} = g_{best}$

An excellent simplified description of the PSO algorithm can be described as follows [23]:

**Step 1:** Define the problem space and set the boundaries, i.e. the acceptable limits of the controller parameters.
**Step 2:** Initialize an array of particles with random positions and their associated velocities inside the problem space. These particle positions represent the initial set of solutions.
**Step 3:** Check if the current position is inside the problem space or not. If not, adjust the positions so as to be inside the problem space.
**Step 4:** Evaluate the fitness value of each particle.
**Step 5:** Compare the current fitness value with the particles' previous best value ($pbest_i$). If the current fitness value is better, then assign the current fitness value to $pbest_i$ and assign the current coordinates to $pbestx_i$ coordinates.
**Step 6:** Determine the current global minimum among particle's best position.
**Step 7:** If the current global minimum is better than *gbest*, then assign the current global minimum to *gbest* and assign the current coordinates to *gbestx* coordinates.
**Step 8:** Change the velocities.
**Step 9:** Move each particle to the new position and return to Step 3.
**Step 10:** Repeat **Step 3**–**Step 9** until a stopping criteria is satisfied.

### 4.2. Imperialist competitive algorithm

The ICA is a new heuristic algorithm for global optimization searches that is based on imperialistic competition. The ICA, similar to other heuristic algorithms such as PSO and GA, starts with an initial population that is called a country. The initial population is divided into 2 types of colonies and imperialists, which together organize empires. The introduced evolutionary algorithm is constituted by imperialistic competition among these empires. During times of competition, the weak empires fall and the strong empires take possession of their colonies. Finally, this competition converges to a state in which

the colonies have the same cost function value, called the imperialist, and there is only one empire. After all of the colonies are divided among the imperialists and the initial empires are created, these colonies move toward their related imperialist state as an assimilation policy [24]. The movement of a colony toward the imperialist is shown in Fig. 1, where $d$ is the distance between the colonies and the imperialist, and $\theta$ and $x$ represent random numbers with uniform distribution, as given in (30).

$$x \approx U(0, \beta \times d), \ \theta \approx U(-\gamma, \gamma) \tag{30}$$

In the above equation, the terms $\beta$ and $\gamma$ describe parameters that modify the area that colonies randomly search around the imperialist. The total cost of all of the empires can be computed from (31). More descriptions about the ICA and the pseudocode of the ICA can be found in [24].

$$T.C.n = Cost(imperialist_n) + \zeta_{ica} mean\{Cost(\text{colonies of empire}_n)\} \tag{31}$$

An excellent simplified description of the ICA algorithm can be described as follows [24]:

- **Step 1**: Select some random points on the function and initialize the empires.
- **Step 2**: Move the colonies toward their relevant imperialist (Assimilating).
- **Step 3**: If there is a colony in an empire which has lower cost than that of imperialist, exchange the positions of that colony and the imperialist.
- **Step 4**: Compute the total cost of all empires (Related to the power of both imperialist and its colonies).
- **Step 5**: Pick the weakest colony (colonies) from the weakest empire and give it (them) to the empire that has the most likelihood to possess it (Imperialistic competition).
- **Step 6**: Eliminate the powerless empires.
- **Step 7**: If there is just one empire, stop, if not go to 2.

The ICA, as a new heuristic algorithm, is used in multiple applications, such as PID controller designing, optimal placement of FACTS devices, economic load dispatch of power systems, power system stabilization, or harmonic elimination in multilevel inverters.

In this paper, the PSO and ICA is used to obtain the optimal values of the supplementary controller parameters of a novel UPFC.

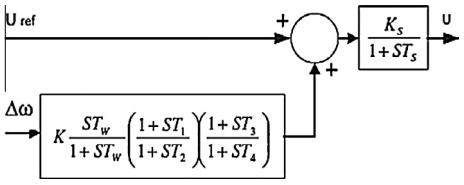


**Figure 3** Proposed UPFC with lead–lag controller.

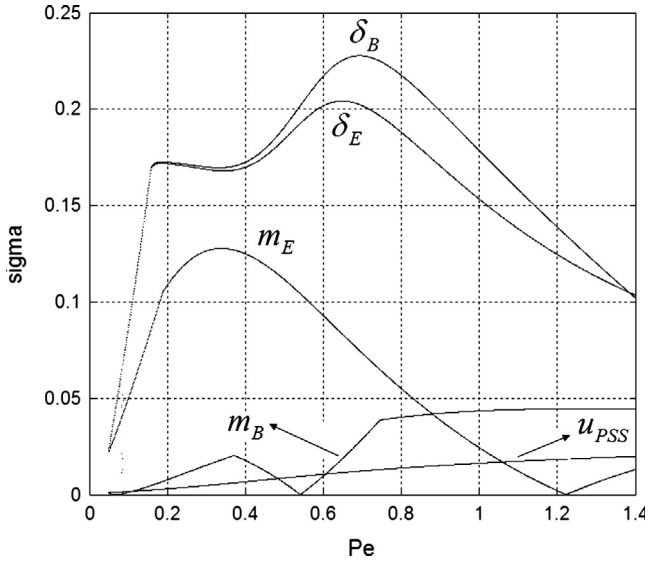


**Figure 4** Minimum singular value with all stabilizers at $Q_e = -0.4$.

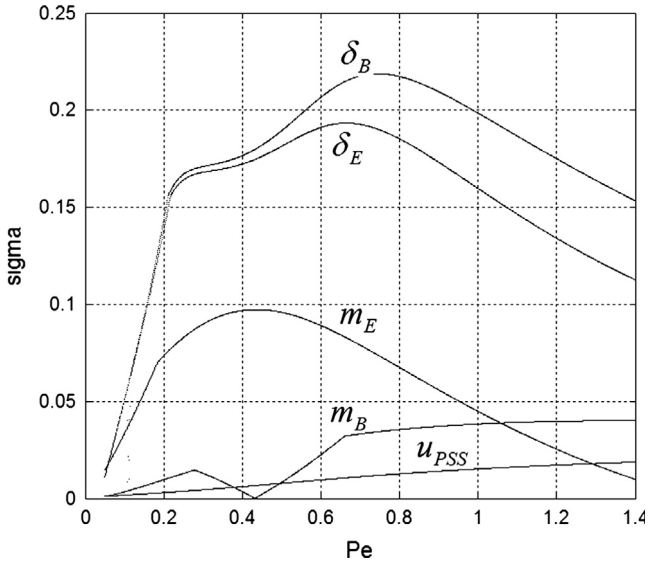


**Figure 5** Minimum singular value with all stabilizers at $Q_e = 0.0$.

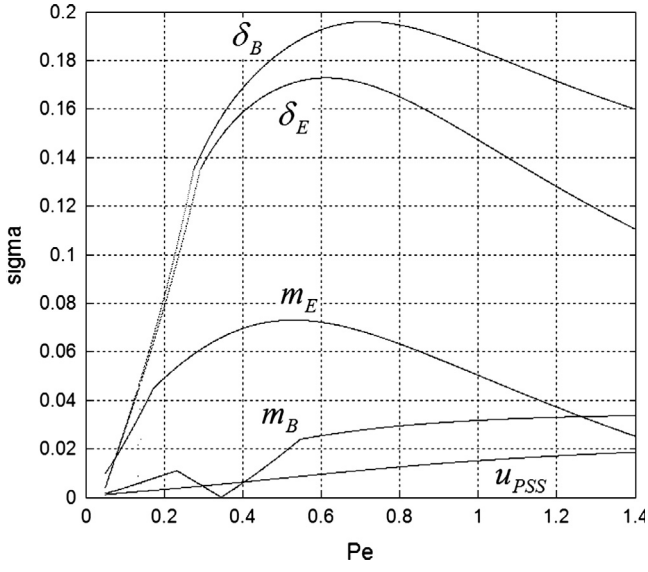


**Figure 6** Minimum singular value with all stabilizers at $Q_e = 0.4$.

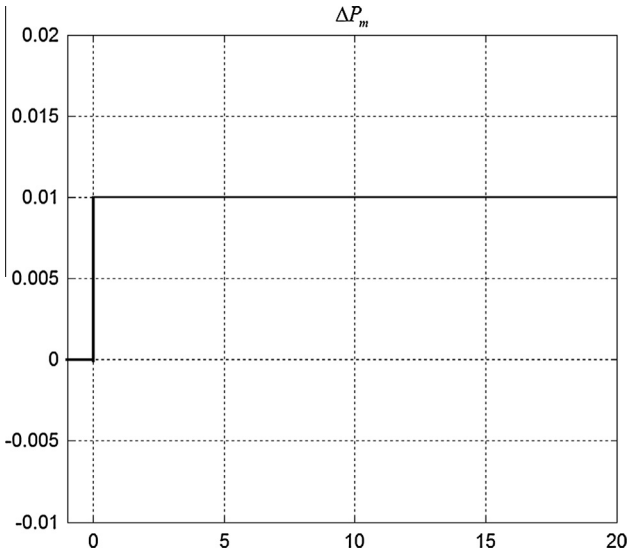


**Figure 7** Step duration in mechanical power.

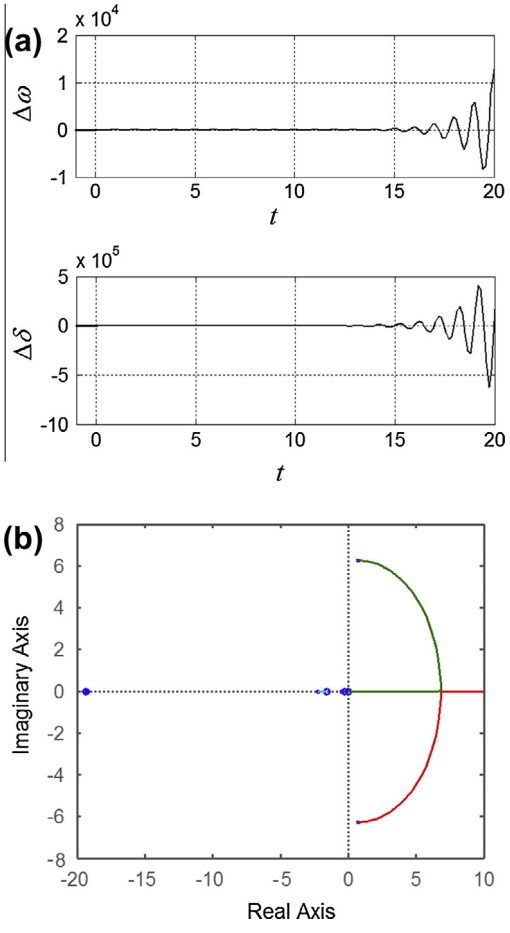


**Figure 8** Light loading without controller. (a) Speed division and load angle division. (b) Root locus diagram.

## 5. PSS and UPFC controllers

The PSS structure to be considered is the very widely used lead-lag controller, whose transfer function is:

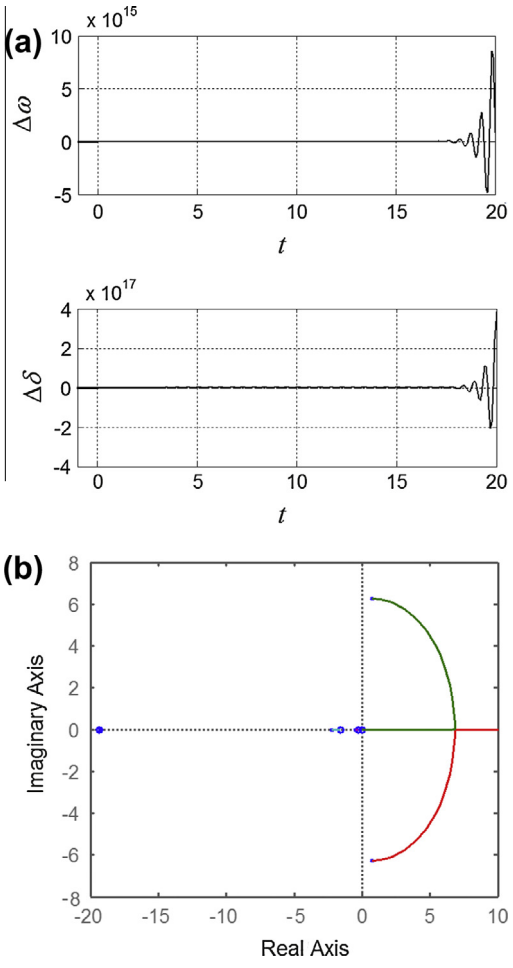


**Figure 9** Normal loading without controller. (a) Speed division and load angle division. (b) Root locus diagram.

$$u_{PSS} = K\frac{sT_w}{1+sT_w}\left(\frac{1+sT_1}{1+sT_2}\right)\left(\frac{1+sT_3}{1+sT_4}\right)\Delta\omega \tag{32}$$

The UPFC damping controllers are of the structure shown in Fig. 3, where u can be $m_E$, $m_B$, $\delta_E$ or $\delta_B$.

### 5.1. Controllability measure

To measure the controllability of the EM mode by a given input (control signal), the singular value decomposition (SVD) is employed. The matrix $B$ can be written as $B = [b_1 b_2 b_3 b_4 b_5]$ where $b_i$ is a column vector corresponding to the $i$th input.

The minimum singular value, $\sigma_{\min}$, of the matrix $[\lambda I - A\, b_i]$ indicates the capability of the $i$th input to control the mode associated with the eigenvalue $\lambda$. Actually, the higher the $\sigma_{\min}$, the higher the controllability of this mode by the input considered. As such, the controllability of the EM mode can be examined with all inputs in order to identify the most effective one to control the mode [23].

### 5.2. Proposed UPFC controller design using PSO and ICA

To acquire an optimal combination, this paper employs PSO and ICA to improve optimization synthesis and find the global

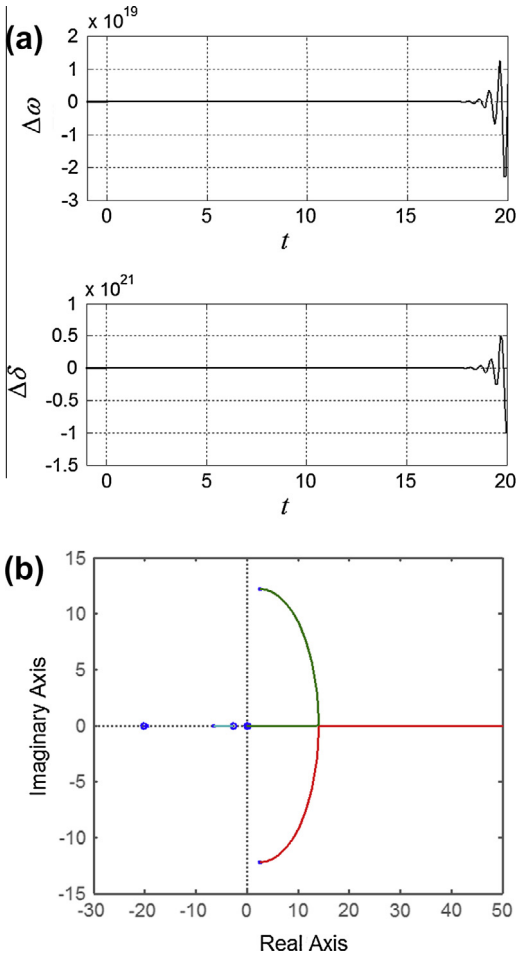


**Figure 10** Heavy loading without controller. (a) Speed division and load angle division. (b) Root locus diagram.

optimum value of fitness function. For our optimization problem, an integral of time multiplied absolute value of the error is taken as the objective function. The objective function is defined as follows [25]:

$$J = \int_0^{t_{sim}} t|\Delta\omega|dt \tag{33}$$

In the above equations, $t_{sim}$ is the time range of simulation and $N_p$ is the total number of operating points for which the optimization is carried out. For objective function calculation, the time-domain simulation of the power system model is carried out for the simulation period. It is aimed to minimize this objective function in order to improve the system response in terms of the settling time and overshoots. The design problem can be formulated as the following constrained optimization problem, where the constraints are the controller parameters bounds [11,25]:

Minimize J

$$\text{Subject to : } K^{\min} \leqslant K \leqslant K^{\max}$$
$$T_1^{\min} \leqslant T_1 \leqslant T_1^{\max}$$
$$T_2^{\min} \leqslant T_2 \leqslant T_2^{\max}$$
$$T_3^{\min} \leqslant T_3 \leqslant T_3^{\max}$$
$$T_4^{\min} \leqslant T_4 \leqslant T_4^{\max}$$

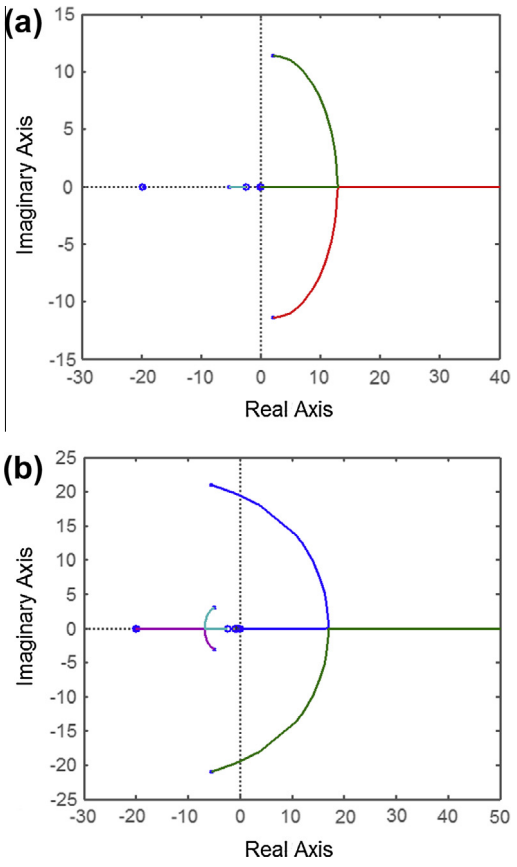


**Figure 11** Root locus diagram in the normal loading. (a) Before adding controller. (b) After adding controller.

Typical ranges of the optimized parameters are [0.01–100] for $K$ and [0.01–2] for $T_1$, $T_2$, $T_3$ and $T_4$. The proposed approach employs PSO and ICA algorithms to solve this optimization problem and search for an optimal or near optimal set of controller parameters. The optimization of UPFC controller parameters is carried out by evaluating the objective function as given in Eq. (33), which considers a multiple of operating conditions. The operating conditions are considered as:

- Case 1: $P_e = 0.80$ pu, $Q_e = 0.114$ pu. (Nominal loading).
- Case 2: $P_e = 0.2$ pu, $Q_e = 0.01$. (Light loading).
- Case 3: $P_e = 1.20$ pu, $Q_e = 0.4$. (Heavy loading).

## 6. Simulation result

### 6.1. Controllability measure

SVD is employed to measure the controllability of the EM mode from each of the five inputs: $u_{PSS}$, $m_E$, $m_B$, $\delta_E$, and $\delta_B$. The minimum singular value, $\sigma_{\min}$, is estimated over a wide range of operating conditions. For SVD analysis, $P_e$ ranges from 0.05 to 1.4 pu and $Q_e = [-0.4, 0, 0.4]$. At each loading condition, the system model is linearized, the EM mode is identified, and the SVD-based controllability measure is implemented.

For comparison purposes, the minimum singular value for all inputs at $Q_e = -0.4$, 0.0 and 0.4 pu is shown in Figs. 4–6, respectively. From these figures, the following can be noticed:

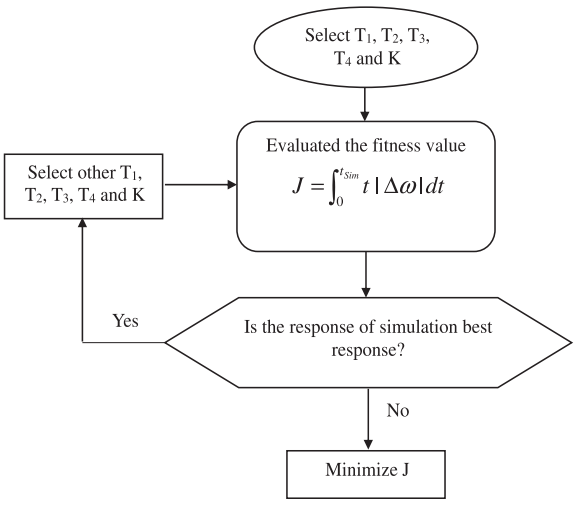


**Figure 12** Flowchart of the proposed design process for UPFC damping controllers.

**Table 1** The optimal parameter of the proposed controllers.

| | | Controller parameters | | | | |
|---|---|---|---|---|---|---|
| | | $T_1$ | $T_2$ | $T_3$ | $T_4$ | $K$ |
| Light loading | PSO | 1.6157 | 1.2947 | 0.8038 | 0.8677 | 3.8721 |
| | ICA | 0.0554 | 0.0405 | 1.3941 | 1.3838 | 4.6523 |
| Nominal loading | PSO | 0.4009 | 1.1307 | 0.4895 | 1.0799 | 77.4544 |
| | ICA | 0.5461 | 1.0678 | 0.3717 | 1.1381 | 74.5505 |
| Heavy loading | PSO | 1.3300 | 0.9176 | 0.2833 | 1.4662 | 47.4357 |
| | ICA | 1.9964 | 1.8287 | 0.2824 | 1.0467 | 45.0005 |

- EM mode controllability via $\delta_B$ is always higher than that of any other input.
- The capabilities of $\delta_B$ and $\delta_E$ to control the EM mode is higher than that of PSS.
- Except PSS, all control signals in the normal load condition is more controllable than the light and heavy load conditions.
- Approximately, the EM mode is more controllable whit $m_E$, $m_B$, $\delta_E$, and $\delta_B$ than the PSS.

### 6.2. Design of damping stabilizers

Linearized model of case study system Fig. 1 with showed parameters in Appendix A and $K$ parameters showed in Appendix B has been simulated with MATLAB/SIMULINK. In order to examine the robustness of the damping controllers to a step load perturbation, it has been applied.

It has been applied a step duration in mechanical power ($\Delta P_m$ = 0.01 pu) to the system of Fig. 2. Fig. 7 shows the step duration in mechanical power.

The reference system has 4 inputs; damping input signal in Figs. 4–6 has been added to the most effective input $\delta_B$ calculated by SVD technique.

Figs. 8–10 show the dynamic responses of $\Delta\omega$ and $\Delta\delta$ with different operating conditions without controller and Root locus diagram for $\delta_B$ input control signal. It is clear that the open loop system is unstable. In other words, without controller system is not stable.

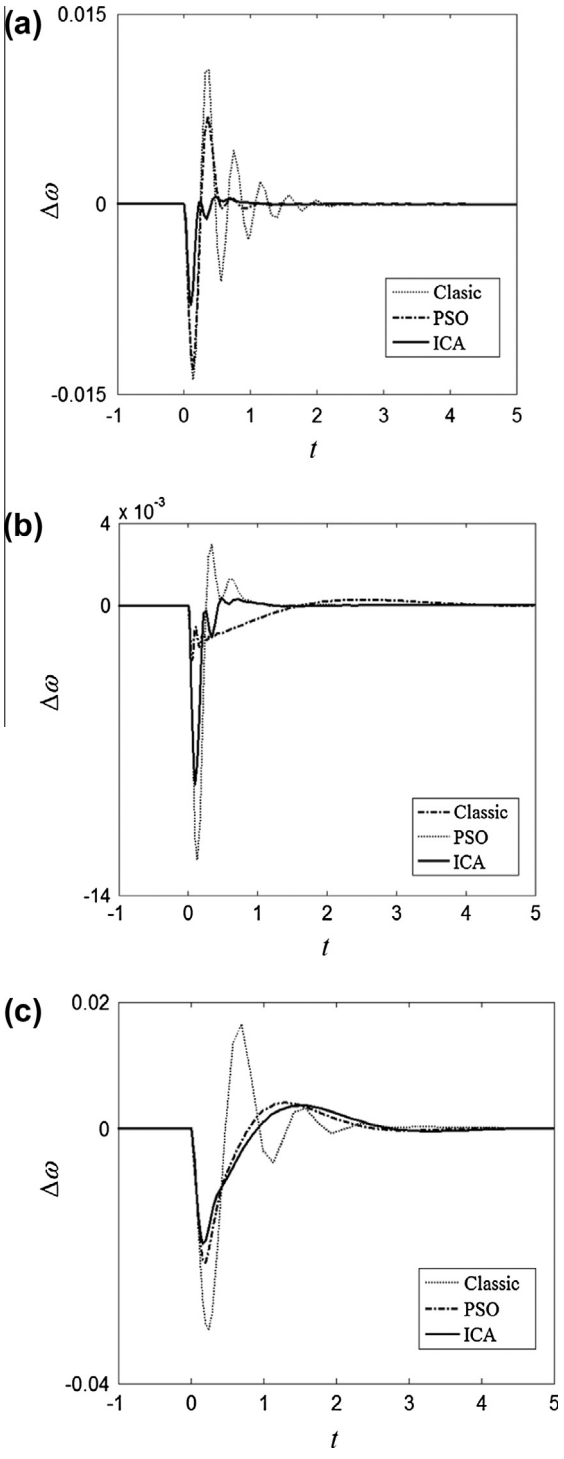


**Figure 13** Dynamic responses of $\Delta\omega$ with input control signal $\delta_B$. (a) Heavy loading. (b) Normal loading. (c) Light loading.

Fig. 11 shows the difference between Root locus diagram before adding the controller and after adding the controller. It is clear that the open loop system is unstable but the proposed controller stabilizes the system. It is obvious that the all unstable poles have been shifted to the left in s-plane and the system damping is greatly improved.

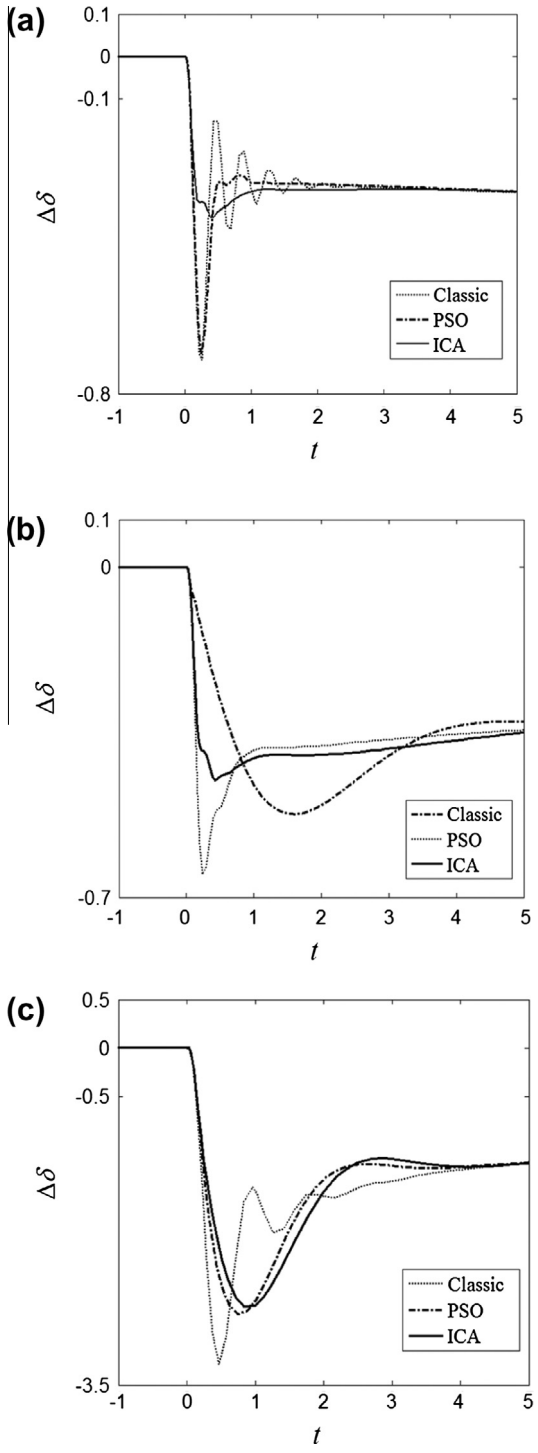


**Figure 14** Dynamic responses of $\Delta\delta$ with input control signal $\delta_B$. (a) Heavy loading. (b) Normal loading. (c) Light loading.

In order to acquire better performance and optimal response of controller, PSO and ICA algorithms are used. It should be noted that mentioned algorithms are run several times and then optimal set of UPFC controller parameters is selected. Fig. 12 shows the fitness function evaluation process contains an inner loop.

The final values of the optimized parameters with objective function, $J$, are given in Table 1.

To assess the effectiveness and robustness of the proposed controllers, the performance of the proposed controller under transient conditions is verified by applying a three-phase fault at $t = 0$ s, at the middle of the one transmission line. The disturbance is cleared by permanent tripping of the faulted line. It can be inferred that the UPFC based damping controller provide satisfactory dynamic performance at the nominal operating condition with objective function. It is extremely important to investigate the effect of variation of the loading condition on the dynamic performance of the system. The speed deviation of generator at nominal, light and heavy loading conditions due to designed controller based on the $\delta_B$ is shown in Figs. 13 and 14.

The performance of the proposed methods is compared with classical method. It can be seen that the ICA based designed controller achieves good robust performance, provides superior damping in comparison with the PSO and classical method; because the speed deviation has been damped with minimum settling time at and minimum overshoot and under shoot for ICA algorithm.

## 7. Conclusions

In this paper, the dynamic model of UPFC, which consist of two shunt converters and a series capacitor, has been obtained. Simulation results operated by MATLAB/SIMULINK show that response of system without using the controller is unstable. For dynamic stability improvement, lead-lag controller has been used. SVD has been employed to evaluate the EM mode controllability to PSS and the four UPFC control signals. It has been shown that the EM mode is most strongly controlled via $\delta_B$ for a wide range of loading conditions. Classical and intelligent techniques have been used to enhance the dynamic stability. The simulation results show that the proposed controller has good performance on damping low frequency oscillations and improves the transient stability under different operating conditions. It is considered that ICA algorithm achieves good robust performance.

## Appendix A

System parameters:

| | | | |
|---|---|---|---|
| Generator | $M = 8$ MJ/MVA | $T'_d = 5.044$ s | $X_d = 1$ pu |
| | $X_q = 0.6$ pu | $X'_d = 0.3$ pu | $D = 0$ |
| Excitation system | | $K_a = 10$ | $T_a = 0.05$ s |
| Transformers | | $X_1 = 0.1$ pu | $X_E = 0.1$ pu |
| | | $X_B = 0.1$ pu | |
| Transmission line | | $X_2 = 1$ pu | |
| Operating condition | | $P = 0.8$ pu | $V_b = 1$ pu |
| | | $V_S = 1$ pu | |
| DC link parameter | | $V_{DC} = 2$ pu | $C_{DC} = 1$ pu |
| UPFC parameter | $X_{Se} = 0.124$ pu | $m_B = 1.0040$ | $\delta_B = 66.6297$ |
| | | $m_E = 1.0185$ | $\delta_E = 60.1777$ |
| | | $K_S = 1$ | $T_S = 0.05$ |

## Appendix B

$K$ parameters:

$$K_1 = (V_{Sd} - X'_d I_{1q})\left(-V_b \sin(\delta)\frac{X_{t4}}{X_{se}X_{d\sum}}\right) + \left(V_{Sq} + X_q I_{1d}\right)\left(V_b \cos(\delta)\frac{X_{t7}}{X_{se}X_{q\sum}}\right)$$

$$K_2 = \left(1 - \frac{X'_d X_{t1}}{X_{se}X_{d\sum}}\right) I_{1q} + \frac{X_{t1}}{X_{se}X_{d\sum}} V_{Sd}$$

$$K_3 = 1 + (X_d - X'_d)\frac{X_{t1}}{X_{Se}X_{d\sum}}$$

$$K_4 = -\frac{X_{t4}(X_d - X'_d)}{2X_{Se}X_{d\sum}} V_b \sin(\delta)$$

$$K_5 = \frac{V_{Sd}X_q X_{t7} V_b \cos(\delta)}{V_S X_{se} X_{q\sum}} + \frac{V_{sq}X'_d X_{t4} V_b \sin(\delta)}{V_S X_{se} X_{d\sum}}$$

$$K_6 = \frac{V_{sq}}{V_S}\left(1 - \frac{X'_d X_{t1}}{X_{se}X_{d\sum}}\right)$$

$$K_7 = \frac{3(X_{2d} m_E \cos(\delta_E) + X_{4d} m_B \cos(\delta_B))}{4C_{dc}X_{d\sum}} V_b \sin(\delta) - \frac{3(X_{1q} m_E \sin(\delta_E) + X_{2q} m_B \sin(\delta_B))}{4C_{dc}X_{q\sum}} V_b \cos(\delta)$$

$$K_8 = \frac{3}{4C_{dc}X_{d\sum}}(m_E \cos(\delta_E) X_{1d} + m_B \cos(\delta_B) X_{Bd})$$

$$K_9 = -\frac{3}{4C_{dc}}\frac{m_E \sin(\delta_E)}{2X_{d\sum}}[m_E \cos(\delta_E) X_{EEd} + m_B \cos(\delta_B) X_{BEd}] - \frac{3}{4C_{dc}}\frac{m_B \sin(\delta_B)}{2X_{d\sum}}[-m_E \cos(\delta_E) X_{EBd} + m_B \cos(\delta_B) X_{BBd}] - \frac{3}{4C_{dc}}\frac{m_E \sin(\delta_E)}{2X_{q\sum}}[m_E \cos(\delta_E) X_{EEq} + m_B \cos(\delta_B) X_{BEq}]$$

$$K_{Pdc} = (V_{Sd} - X'_d I_{1q})(m_E \sin(\delta_E)\frac{X_{t2}}{2X_{se}X_{d\sum}} - m_B \sin(\delta_B)\left(\frac{X_{t3}}{2X_{se}X_{d\sum}}\right) + (V_{Sq} + X_q I_{1d})\left(m_E \cos(\delta_E)\frac{X_{t5}}{2X_{se}X_{q\sum}} + m_B \cos(\delta_B)\frac{X_{t6}}{2X_{se}X_{q\sum}}\right)$$

$$K_{PE} = (V_{Sd} - X'_d I_{1q})\left(\sin(\delta_E) \cdot V_{dc}\frac{X_{t2}}{2X_{se}X_{d\sum}}\right) + (V_{Sq} + X_q I_{1d})\left(\cos(\delta_E) \cdot V_{dc}\frac{X_{t5}}{2X_{se}X_{q\sum}}\right)$$

$$K_{P\delta_E} = (V_{Sd} - X'_d I_{1q})\left(m_E \cos(\delta_E) \cdot V_{dc}\frac{X_{t2}}{2X_{se}X_{d\sum}}\right) + \left(V_{Sq} + X_q I_{1d}\right)\left(-m_E \sin(\delta_E) \cdot V_{dc}\frac{X_{t5}}{2X_{se}X_{q\sum}}\right)$$

$$K_{PB} = (V_{Sd} - X'_d I_{1q})\left(-\sin(\delta_B) \cdot V_{dc}\frac{X_{t3}}{2X_{se}X_{d\sum}}\right) + \left(V_{Sq} + X_q I_{1d}\right)\left(\cos(\delta_B) \cdot V_{dc}\frac{X_{t6}}{2X_{se}X_{q\sum}}\right)$$

$$K_{P\delta_B} = (V_{Sd} - X'_d I_{1q})\left(m_B \cos(\delta_B) \cdot V_{dc}\frac{X_{t3}}{2X_{se}X_{d\sum}}\right) + (V_{Sq} + X_q I_{1d})\left(-m_B \sin(\delta_B) \cdot V_{dc}\frac{X_{t6}}{2X_{se}X_{q\sum}}\right)$$

$$K_{qdc} = \frac{(X_d - X'_d)}{2X_{Se}X_{d\sum}}(X_{t2} m_E \sin(\delta_E) - X_{t3} m_B \sin(\delta_B))$$

$$K_{qE} = \frac{X_{t2}(X_d - X'_d)}{2X_{Se}X_{d\sum}} \sin(\delta_E) V_{dc}$$

$$K_{q\delta_E} = \frac{X_{t2}(X_d - X'_d)}{2X_{Se}X_{d\sum}} m_E \cos(\delta_E) V_{dc}$$

$$K_{qB} = -\frac{X_{t3}(X_d - X'_d)}{2X_{Se}X_{d\sum}} \sin(\delta_B) V_{dc}$$

$$K_{q\delta_B} = -\frac{X_{t3}(X_d - X'_d)}{2X_{Se}X_{d\sum}} m_B \cos(\delta_B) V_{dc}$$

$$K_{Vdc} = \frac{V_{sd}}{V_S} X_q\left(m_E \cos(\delta_E)\frac{X_{t5}}{2X_{se}X_{q\sum}} + m_B \cos(\delta_B)\frac{X_{t6}}{2X_{se}X_{q\sum}}\right) - \frac{V_{sq}}{V_S} X'_d\left(m_E \sin(\delta_E)\frac{X_{t2}}{2X_{se}X_{d\sum}} - m_B \sin(\delta_B)\frac{X_{t3}}{2X_{se}X_{d\sum}}\right)$$

$$K_{VqE} = \frac{V_{sd}}{V_S} X_q\left(\cos(\delta_E) \cdot V_{dc}\frac{X_{t5}}{2X_{se}X_{q\sum}}\right) - \frac{V_{sq}}{V_S} X'_d\left(\sin(\delta_E) \cdot V_{dc}\frac{X_{t2}}{2X_{se}X_{d\sum}}\right)$$

$$K_{V\delta_E} = -\frac{V_{sd}}{V_S} X_q\left(m_E \sin(\delta_E) \cdot V_{dc}\frac{X_{t5}}{2X_{se}X_{q\sum}}\right) - \frac{V_{sq}}{V_S} X'_d\left(m_E \cos(\delta_E) \cdot V_{dc}\frac{X_{t2}}{2X_{se}X_{d\sum}}\right)$$

$$K_{V\delta_E} = -\frac{V_{sd}}{V_S} X_q\left(m_E \sin(\delta_E) \cdot V_{dc}\frac{X_{t5}}{2X_{se}X_{q\sum}}\right) - \frac{V_{sq}}{V_S} X'_d\left(m_E \cos(\delta_E) \cdot V_{dc}\frac{X_{t2}}{2X_{se}X_{d\sum}}\right)$$

$$K_{V\delta_B} = -\frac{V_{sd}}{V_S}X_q\left(m_B\sin(\delta_B)\cdot V_{dc}\frac{X_{t6}}{2X_{se}X_{q\sum}}\right) + \frac{V_{sq}}{V_S}X'_d\left(m_B\cos(\delta_B)\cdot V_{dc}\frac{X_{t3}}{2X_{se}X_{d\sum}}\right)$$

$$K_{CE} = \frac{3}{4C_{dc}}\left(\cos(\delta_E)I_{Ed}+\sin(\delta_E)I_{Eq}\right) + \frac{3m_E}{8C_{dc}}\sin(\delta_E)\cos(\delta_E)V_{dc}\left(\frac{X_{EEd}}{X_{d\sum}}+\frac{X_{EEq}}{X_{q\sum}}\right) + \frac{3m_B}{4C_{dc}}\left(\sin(\delta_E)\cos(\delta_B)V_{dc}\frac{X_{BEd}}{2X_{d\sum}}+\sin(\delta_B)\cos(\delta_E)V_{dc}\frac{X_{BEq}}{2X_{q\sum}}\right)$$

$$K_{C\delta_E} = \frac{3m_E}{4C_{dc}}\left(-\sin(\delta_E)I_{Ed}+\cos(\delta_E)I_{Eq}\right) + \frac{3m_E^2V_{dc}}{8C_{dc}}\left(\frac{X_{EEd}}{X_{d\sum}}\cos^2(\delta_E)-\frac{X_{EEq}}{X_{q\sum}}\sin^2(\delta_E)\right) + \frac{3m_Em_BV_{dc}}{8C_{dc}}\left(\frac{X_{BEd}}{X_{d\sum}}\cos(\delta_E)\cos(\delta_B)-\frac{X_{BEq}}{X_{q\sum}}\sin(\delta_E)\sin(\delta_B)\right)$$

$$K_{CB} = \frac{3}{4C_{dc}}\frac{\sin(\delta_B)V_{dc}}{2X_{d\sum}}(-m_E\cos(\delta_E)\cdot X_{EBd}+m_B\cos(\delta_B)\cdot X_{BBd}) + \frac{3}{4C_{dc}}\frac{\cos(\delta_B)V_{dc}}{2X_{q\sum}}\times(m_E\sin(\delta_E)\cdot X_{EBq}+m_B\sin(\delta_B)\cdot X_{BBq}) + \frac{3}{4C_{dc}}\left(\cos(\delta_B)I_{Bd}+\sin(\delta_B)I_{Bq}\right)$$

$$K_{C\delta_B} = \frac{3}{4C_{dc}}\frac{m_B\cos(\delta_B)V_{dc}}{2X_{d\sum}}\times(-m_E\cos(\delta_E)\cdot X_{EBd}+m_B \times\cos(\delta_B)\cdot X_{BBd}) + \frac{3}{4C_{dc}}\frac{m_B\sin(\delta_B)V_{dc}}{2X_{q\sum}}\times(-m_E\sin(\delta_E) \cdot X_{EBq}-m_B\sin(\delta_B)\cdot X_{BBq}) + \frac{3}{4C_{dc}}(\cos(\delta_B)I_{Bd} + \sin(\delta_B)I_{Bq})$$

## References


[1] Banaei Mohamad Reza, Golizadeh. Designing of UPFC controller for damping of electromechanical oscillations using imperialist competitive algorithm. Int Rev Appl Contr 2011;4(4):553–61.

[2] Chen CL, Hsu YY. Coordinated synthesis of multimachine power system stabilizer using an efficient decentralized modal control (DMC) algorithm. IEEE Trans Power Syst 1987;9(3):543–51.

[3] Gibbard MJ. Co-ordinated design of multimachine power system stabilisers based on damping torque concepts. IEE Proc Pt C 1988;135(4):276–84.

[4] Klein M, Le LX, Rogers GJ, Farrokhpay S, Balu NJ. $H_\infty$ damping controller design in large power systems. IEEE Trans Power Syst 1995;10(1):158–66.

[5] Samarasinghe VGDC, Pahalawaththa NC. Damping of multimodal oscillations in power systems using variable structure control techniques. IEE Proc Gener Transm Distrib 1997;144(3):323–31.

[6] Abdel-Magid YL, Abido MA, Al-Baiyat S, Mantawy AH. Simultaneous stabilization of multimachine power systems via genetic algorithms. IEEE Trans Power Syst 1999;14(4):1428–39.

[7] Abido MA. Particle swarm optimization for multimachine power system stabilizer design. In: IEEE power eng society summer meeting, 15–19 July 2001, vol. 3; 2001. p. 1346–51.

[8] Abido MA, Abdel-Magid YL. Radial basis function network based power system stabilizers for multimachine power systems. In: Int conf neural networks, 9–12 June 1997, vol. 2; 1997. p. 622–6.

[9] Mahran AR, Hogg BW, El-Sayed ML. Co-ordinated control of synchronous generator excitation and static VAR compensator. IEEE Trans Energy Convers 1992;7:615–22.

[10] Banaei MR, Kami A. Interline power flow controller (IPFC) based damping recurrent neural network controllers for enhancing stability. Energy Convers Manage 2011:2629–36.

[11] Al-Awami AliT, Abdel-Magid YL, Abido MA. A particle-swarm-based approach of power system stability enhancement with unified power flow controller. Electr Power Energy Syst 2007;29:251–259.

[12] Mishra S, Hota PK, Mohanty P. A neuro fuzzy based unified power flow controller for improvement of transient stability performance. IE (I) J 2003:148–53.

[13] Kalyani Radha P, Venayagamoorthy Ganesh K. Two separately continually online trained neurocontrollers for a unified power flow controller. In: Proceedings of international conference on intelligent sensing and information processing. (IEEE Cat No 04EX783); 2004. p. 243–8.

[14] Keri AJF, Lombard X, Edris AA. Unified power flow controller: modeling and analysis. IEEE Trans Power Deliv 1999;14(2):648–54.

[15] Wang HF. Application of modeling UPFC into multi-machine power system. IEE Proc Gener Transm Distrib 1999;146(3):306–12.

[16] Rouco L. Coordinated design of multiple controllers for damping power system oscillation. Electr Power Energy Syst 2001:517–30.

[17] Pal BC. Robust damping of inter area oscillations with unified power flow controller. IEE Proc Gener Transm Distrib 2002;149(6):733–8.

[18] Wang HF. Damping function of unified power flow controller. IEEE Trans Proc-Gener Trans Distrib 1999;146(1):81–7.

[19] Wang HF. Application of modeling UPFC into multi-machine power systems. IEE Proc Gener Transm Distrib 1999;146(3):306–12.

[20] Abido MA, Al-Awami Ali T, Abdel-Magid YL. Simultaneous design of damping controllers and internal controllers of a unified power flow controller. In: Power engineering society general meeting. Montreal: IEEE; 2006.

[21] Sadigh Arash Khoshkbar, Hagh Mehrdad Tarafdar, Sabahi Mehran. Unified power flow controller based on two shunt converters and a series capacitor. Electric Power Syst Res 2010;80:1511–9.

[22] Kennedy J, Eberhart R. Particle swarm optimization. In: Proc IEEE intl conf neural networks, vol. 4; 1995. p. 1942–8.

[23] Al-Awami1 Ali T, Abido Mohammed A, Abdel-Magid Youssef L. Swarm intelligence, focus on ant and particle swarm optimization. Publisher I-Tech Education and Publishing; 2007.

[24] Atashpaz-Gargari Esmaeil, Lucas Caro. Imperialist competitive algorithm: an algorithm for optimization inspired by imperialistic competition. In: IEEE congress on; 2007. p. 4661–7.

[25] Shayeghi H, Shayanfar HA, Jalilzadeh S, Safari A. Tuning of damping controller for UPFC using quantum particle swarm optimizer. Energy Convers Manage 2010;51:2299–306.

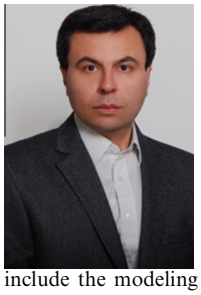

**Mohamad Reza Banaei** was born in Tabriz, Iran. He received his M.Sc. degree from the Poly Technique University of Tehran, Iran, in control engineering in 1999 and his Ph.D. degree from the electrical engineering faculty of Tabriz University in power engineering in 2005. He is an Associate Professor in the Electrical Engineering Department of Azarbaijan Shahid Madani University, Iran, which he joined in 2005. His main research interests include the modeling and controlling of power electronic converters, renewable energy, modeling and controlling of FACTS and Custom Power devices and power systems dynamics.

**Seyed-Jalal Seyed-Shenava** was born in Ardabil/Iran. He received his B.Sc. in Electrical Engineering from Tehran University in 1991, and his M.SC. and Ph.D. in Electrical Power Engineering both from TMU (Tarbiat Modares University), Tehran/Iran in 1995 and 2008, respectively. Since 1995, he has been with University of Mohaghegh Ardabili, Ardabil/Iran where he is currently an assistant professor. His research interests are electricity planning, operation and reliability of power systems.

**Parisa Farahbakhsh** was born in Tabriz, Iran, in 1988. She received her B.S. Degree in Power Electrical Engineering from Azarbaijan Shahid Madani University, Tabriz, Iran, in 2010. She received his M.S. degree from University of Mohaghegh Ardabili, Ardabil, Iran, in 2013. Her main research interests include power system control, flexible AC transmission systems (FACTS) and power systems dynamic modeling.